

Collated Studies on Rectifying Circuit on Impact-Based Piezoelectric Energy Harvesting

Nur Amalina Ahmad Nawir¹, Amat Amir Basari^{1,2}, Ng Xue Yan¹

¹*Faculty of Electronic and Computer Engineering, Universiti Teknikal Malaysia Melaka UTeM),
76100 Durian Tunggal, Melaka, Malaysia*

²*Centre for Telecommunication Research & Innovation (CeTRI),
Faculty of Electronic and Computer Engineering, Universiti Teknikal Malaysia Melaka (UTeM),
76100 Durian Tunggal, Melaka, Malaysia.
amat@utem.edu.my*

Abstract—Nowadays, energy consumption for ultra-low power energy such as piezoelectric energy harvester has suffered a very huge power loss when rectifying the generated AC signal into regulated DC voltage. This paper presents a method on enhancing the efficiency of the proposed rectifier circuit on Lead Zirconate Titanate (PZT) piezoelectric disk. The experiment was conducted by actuating the transducer by applying one single impact pulse only from a weight-drop test setup. The aim of this study is to increase the efficiency of the extracted output power from piezoelectric by reducing the power losses during the rectification process. Enhancements were made by identifying factors affecting the generated output power from the transducer. Four different types of rectifier topologies were studied and optimized by varying the level of forward voltage drop, V_f across the diode. The enhancement of the generated output voltage from the harvester was also conducted by altering and specifically designed the mechanical configuration of the disk's supporting base in order to increase the displacement of the piezoelectric strain. The system performances have been analyzed and the resulted data have been plotted into voltage and power curves against the resistive impedance. It was found that the power efficiency of full-wave bridge rectifier constructed with the lowest V_f , is the highest compared to the half-wave and the specialized voltage doubler rectifier.

Index Terms— Energy Harvester, Impact-based Technique, Piezoelectric, Rectifier Circuit, Voltage Doubler.

I. INTRODUCTION

In this millennial era, electricity is becoming essential in everyday life. The rapid growth of civilization, industrialization and technology development has also resulted in the continuous increase of global demand for the electricity. Harvesting energy from natural resources such as photovoltaic [1], geothermal [2], windmills [3] and watermills [4] have been widely used for producing a large scale of electrical power. However, they are leaving a very large footprint to our mother nature. Issues on the attainability of energy sources that can sustain the ecosystem have alarmed numerous researchers in finding the best alternative solutions in providing electricity.

After solar power, kinetic energy offers the highest power density with 50 to 330 $\mu\text{W}/\text{cm}^3$ [5]. Lately, the trends of recycling waste energy such as heat, vibration or radio waves produced by the mechanical vibration from human motion or machines have become popular. Despite the small energy production, it quite significant for powering

electronic devices with low power requirement such as micromechanical system (MEMS) and Wireless Sensor Network (WSN) [6], [7]. Conventionally, these devices are limited by the lifespan of batteries and the difficulties to access for maintenance.

These addressing problems can be resolved effectively by utilizing the vibrations energy by converting it into electricity using appropriate micromechanical-transducer. Among the most popular devices for this type of energy regeneration, piezoelectric-based transducer offers the highest output voltage compared to electrostatic and electromagnetic-based transducer [8]–[10].

Piezoelectric device generates electricity when there is a deformation on the composite crystalline structure, which is mainly consists of Lead Zirconate Titanate (PZT), Barium Titanate, Rochelle salt, quartz and others [11]. This structure can be deformed either by using a continuous vibration (d31-mode), which is normally the transducer in cantilever form or either by using impact force (d33-mode) on top of the material that will generate a pulse signal [12], [13]. Studies show that natural characteristic of the vibration frequency on the environment is in the range of 100Hz. However, it is difficult to find in nature a cantilever beam piezoelectric transducer that achieves resonance frequency below the natural frequency. In order to generate an optimum output power from the piezoelectric, the excitation frequency of the driving surface needs to be operated almost near or matches with the resonance frequency of the material. Meanwhile, for the impact-based excitation, the variables affecting the piezoelectricity is mostly depended on the mass and velocity applied and it can be applied to the low-frequencies application such as human body, which normally generates within 10 to 30 Hz. Therefore, the concept of harvesting raw energy especially from kinetic energy using an impact force instead of continuous vibration on piezoelectric device has become the most promising scheme for powering low-powered device within the ranges of microwatts (μW) to milliwatts (mW) [14], [15].

Nowadays, most of the electronic devices in the market is powered by regulated direct current (DC) voltage sources. However, piezoelectric materials are known to generate an alternating current (AC) voltage when subjected to mechanical stress or vibration. Therefore, the output from the harvester needs to be rectified first from AC form to DC regulated voltage for it to be useful to power up the devices [16]. Numerous studies on the mechanical impact type have been performed by different approaches; free-fall test [17]–

[20], free moving object [21]–[23] and directional stress that are actuated by using hydraulic pressing machine [24]. The papers that had been mentioned before are generally categorized in a short-duration impact loading and most of them are only focusing only on the harvested output power taken directly from the piezoelectric. This type of energy is not suitable to drive any electronic device as there are no rectification and filtration unit in the system. Although there are a lot of researches on the conversion rectifier with the piezoelectric harvester as in [25] and [26], these experiments are based on the vibration technique and the transducers are in cantilever form that actuate at specific frequency.

Therefore, in this paper, a method of enhancing the generated output power from the piezoelectric and reducing the power losses during the conversion of AC to DC signal in the rectification process is demonstrated. The studies are carried out by actuating the transducer by only one impact pulse. The ceramic disk piezoelectric is excited by using weight-drop analysis that applies the force on top of the transducer using the relationship of height, mass and gravitational acceleration. These three parameters are made constant throughout the experiment as the paper focuses on enhancing the harvester power on the harvester management circuit; rectifier, capacitive filter and resistive load. Focusing on the effectiveness of the harvesting circuitry, three important components that affect the output performances of the harvester are analyzed and compared in this study. Lastly, the performance of the power harvested by using different rectifier topologies will be discussed and compared.

II. IMPACT FORCE OF FALLING OBJECT

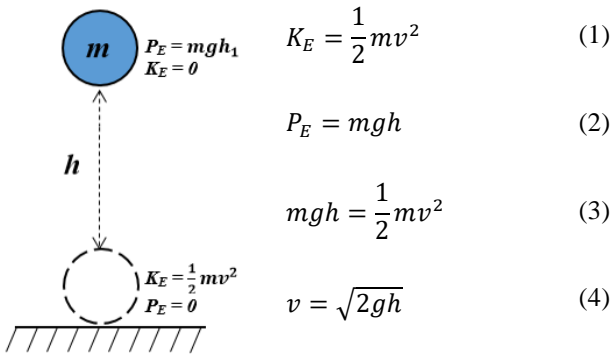


Figure 1: Application of conservations of energy to a free-falling object.

Kinetic energy (K_E) is the energy possessed by all moving object due to the movement or motion when a force is applied. Simply put, if an object is at rest, it does not possess this type of energy. It can be measured by referring to Equation (1), where the kinetic energy of an object is dependent on the two variables; velocity of the object, v and mass, m that is first discovered by Sir Isaac Newton. A small change in velocity is able to affect a huge change on the kinetic energy as both of the variables are directly proportional to it.

Meanwhile, gravitational potential energy (P_E) in Equation (2) is the energy that is stored within an object due to its position relative to the gravitational acceleration, g (9.8 m/s² on Earth). At this position, the object is considered to have zero kinetic energy or known as at rest. The relationship of this two can be referred in Figure 1, where as a force is applied to an object at rest, its potential energy

will be converted into kinetic energy. The initial kinetic energy of the falling object is zero with a high potential energy. Once the object hits the ground, the height will become zero, therefore no potential energy at the ground level. Thus the new equation based on this relationship, Initial $P_E =$ Final K_E can be written as Equation (3). From this equation, the amount of the velocity can be directly calculated when the displacement value of h is known as shown in Equation(4).

$$F = \frac{K_E}{h_2} = \frac{mv^2}{2h_2} \quad (5)$$

The dent on the surface impacted creates an impact depth, h_2 that affect the resulted output force on the piezoelectric based on the Equation (5). In damping condition, the generated impact force is directly proportional to the mass of the object and velocity factors. The deeper the depth, the lesser the impact force on the object. From this mathematical equations, it can be said that the output power produced from the piezoelectric transducer relies on the impact velocity of the object along with the impact force of the object when the kinetic energy and the momentum of the object remains the same [27]. Based on these claims, the generated output power transfer from the transducer to the external load can be elevated by increasing the displacement of the piezoelectric, as illustrated in Figure 2.



Figure 2: The illustration of the strain displacement of the object (a) when the object is detained by a flat surface (b) when the object has a hole beneath it.

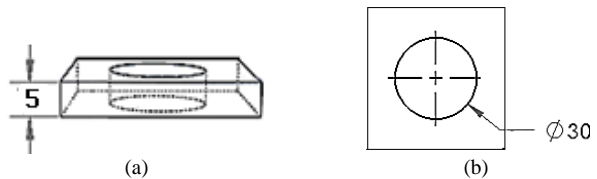


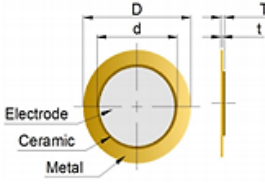
Figure 3: Cross-sectional view of the setting base (a) side view, (b) top view

It can be seen from Figure 2 that the object (in this case the object is referred to the piezoelectric) is assembled on two different setups. In the first condition, Figure 2(a), the object is placed on top of a flat surface bench. This setup arrangement restricts the vertical displacement of the piezoelectric when a force is applied on it. If the displacement of the piezo is detained by the supporting surface, the resulted output voltage from the piezoelectric is going to be affected. Since the generated output voltage from piezoelectric is in sinusoidal form, the signal is normally bound from generating the negative half cycle part. Therefore, in order to overcome this limitation, the piezoelectric is proposed to be set on a supporting base with a hole beneath it. The purpose of this hole is to increase the strain displacement of the piezoelectric vertically and enhance the generated output energy from the piezo. The supporting base is designed specifically based on the proposed transducer with a 30mm hole diameter that will support the 35mm brass diameter of the piezoelectric. The

supporting base has been designed with a dimension of (50 x 50 x 5) mm³ as shown in Figure 3.

III. PIEZOELECTRIC ENERGY HARVESTER & RECTIFIER CIRCUITRY

Table 1
PZT Parameters

Dimensional Drawing	Parameters	Value
	Part Number	7BB-35-3
	Capacitance (nF)	30.0
	Plate, D (mm)	35.0
	Ceramic, a (mm)	25.0
	Electrode, d (mm)	23.0
	Thickness, T (mm)	0.53
	Plate thickness, t (mm)	0.30

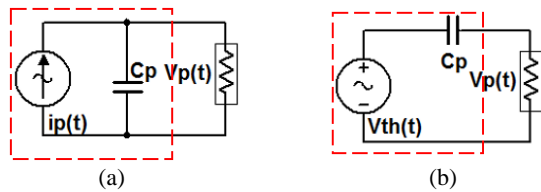


Figure 4: Piezoelectric equivalent schematic diagram (a) Norton, (b) Thevenin [28],[29].

There are two types of piezoelectric composites; PZT and Polyvinylidene Fluoride (PVDF) that are broadly used for generating electricity from kinetic energy. Between these two, the most suitable piezoelectric materials for impact-based application method is determined by their efficiency in producing electrical energy. PVDF has an advantage in term of flexibility when comparing with PZT, which is it is much more brittle than PVDF. However, PZT is able to produce electricity much more efficient than PVDF in general. In this study, a conventional piezoelectric material, ceramic disk PZT was selected for impact-force energy regeneration. The dimensional drawing of unimorph (Murata 7BB-35-3) can be seen from the dimensional drawing in Table 1. Generally, it was constructed with the composition of three important elements; electrode, crystallize ceramic with internal capacitance of 30 nF and brass metal.

Figure 4(a) and (b) show the transducer equivalent circuit diagram (within the red box) that is connected with an external resistive load. Based on Norton theorem, the internal characteristic of the piezoelectric transducer is composed of the transducer’s internal capacitance, c_p that is connected in parallel with the current source as shown in Figure 4(a). The internal capacitance, c_p also can be modeled in series with the voltage source according to the Thevenin theorem as shown in Figure 4(b).

From the schematics, the voltage labeled across the resistor is $V_p(t)$, which indicates that the signal is in time-varying form. Therefore, this AC signal needs to be rectified first before it is able to power up DC power sources electronic equipment. In order to enhance the generated output power from the harvester, several types of uncontrolled rectifier topologies for single-phase circuit have been investigated. Besides, an investigation on the components that affect the performance of the harvester circuit was also conducted involving the characteristic of the diodes and optimum resistive load.

Figure 5 shows the schematic diagram of AC-DC

converter used in the characterizing experiments. The most basic kind of rectifier circuit is the half-wave rectifier, which consists of only one diode to allow only one half of sinewave signals to pass through to the load as shown in Figure 5(a). Unlike the half-wave rectifier, full-wave bridge rectifier, Figure 5(b) can utilize both the negative and the positive portion of the sinewave input signals. These conventional rectifiers normally deliver the output voltage lower than the input due to the losses during rectification. However, a special type of rectifier circuit known as voltage doubler; half-wave in Figure 5(c) and full-wave in Figure 5(d), which are also known as Greinacher and Delon voltage doubler is able to produce an output voltage two times greater than the applied input voltage by storing the charges in the capacitors C_1 and C_2 alternately.

Normally, all of these circuits are used to rectify the signals from a continuous AC sources. However, in this study, the experiments were arranged for only one single impact signal from the weight-drop analysis. The behavior of the harvester and the rectifier circuit will be analyzed and compared. The parameters that affect the output power of the harvester are the diodes characteristic, the rectifier configuration and the external resistive load.

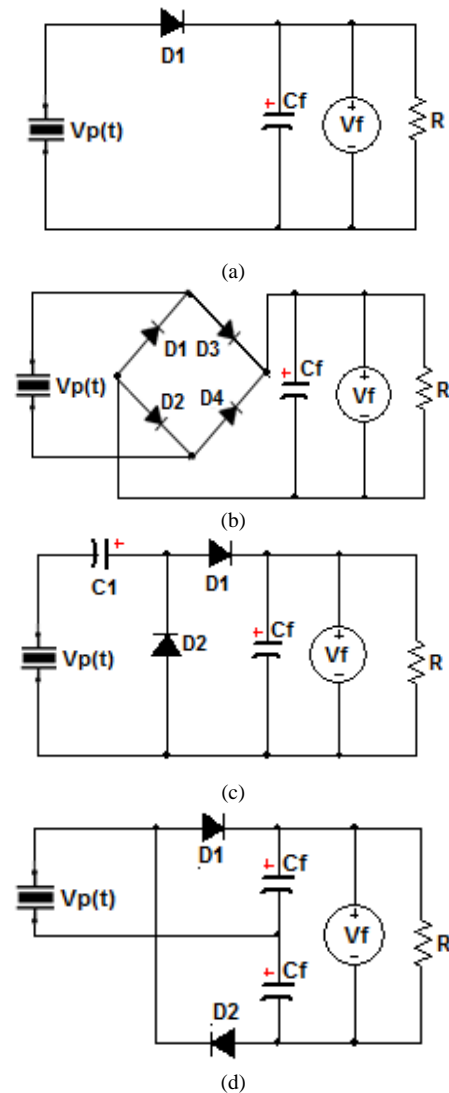


Figure 5: AC-DC converter (a) Half-wave rectifier (b) Full-wave bridge rectifier, (c) Half Wave Voltage Doubler and (d) Full Wave Voltage Doubler.

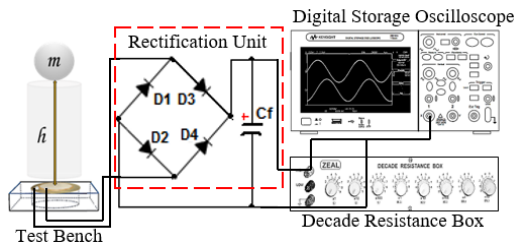


Figure 6: Overall experimental setup block diagram.

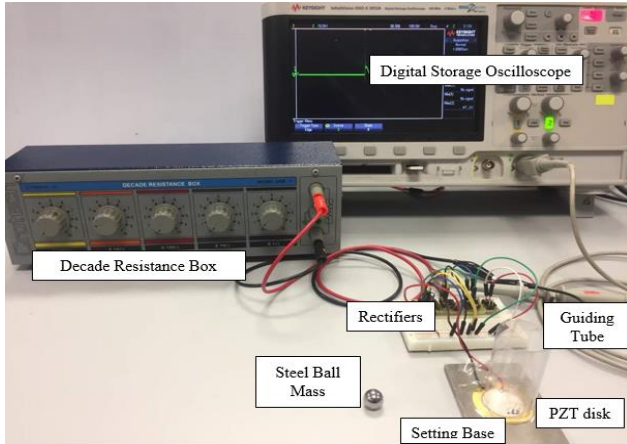


Figure 7: Impact-based piezoelectric energy harvester experimental setup

IV. IMPACT-BASED PIEZOELECTRIC ENERGY HARVESTER EXPERIMENTAL SETUP

The drop test experimental setup was designed and constructed as shown in Figure 6 for characterizing and evaluating the power potential of the transducer. The setup, consisting of a test bench, energy harvesting circuits and the measured signal was acquired by using KEYSIGHT, Digital Storage Oscilloscope (DSO-X 2912A). The ceramic disk piezoelectric transducer, (7BB-35-3) manufactured by Murata Manufacturing Co. Ltd was mounted onto the setting base with a hole of 30 mm in diameter as shown in Figure 7. A wide range decade resistance box, from Cratech UK was used as a load. To give an impact kind of force, a steel ball with 1-gram mass was dropped vertically from the height of 50 mm above the piezoelectric device. A cylinder conducting tube was used as a guiding shield to hit the device precisely and consistently at the spot in order to deliver constant forces. Since, this test was operated manually by the human not by a machine, the experiments for each parameter took place several times. All of the resulted data were calculated. Further, the results from its average were finalized in order to make sure the data taken are reliable and accurate.

As shown in Figure 6, the transducer is connected to the energy harvesting circuit, which consists of rectifier diodes and a capacitive filter before it is connected to a decade resistive box, which acts as a load. Several series of experiment were conducted with the intention of enhancing the generated output power. In the first series of experiments, three different types of diode with different specification; Schottky, Silicon, and Zener were tested as the harvester rectifiers. To evaluate the use of the most efficient diode in a harvester circuitry, the diodes were constructed in a full-wave bridge rectifier as shown in the block diagram. The best performance diode was selected in

the next experiment to study the behavior of different rectifier configuration by changing the configuration with half-wave, full wave voltage doubler and half-wave voltage doubler. Figure 7 shows the actual experimental setup with a numbers of rectifying circuit topologies used in these studies.

V. RESULTS VERIFICATION

Based on the configurations setup in Figure 6 and Figure 7, the studies were conducted and categorized into two sets of experiments. Similar to the previous study, the harvested output voltage from the piezoelectric was in time-varying AC signal. A simple test to verify this claim has been taken place by dropping 1-gram steel ball mass vertically on top of the piezo with the displacement of 50 mm high. The resulted output voltage was obtained in open-circuit connection by directly connecting the harvester to the digital storage oscilloscope and the resulted output signal was captured as shown in Figure 8. From this figure, it can be seen that the generated output signal is in AC form, where it has the positive and negative parts. This result validates the previous statement that the harvested output voltage from piezoelectric is in AC form. The oscilloscope captured and recorded the generated output voltage from the piezo with a sampling time of 100ms in a single run control mode operation. In order to prevent from mistaking the surrounding noise or any external force as the input signal, the oscilloscope has been set to trigger only when it receives a signal higher than 10V. The parameters of the experiments; mass of the steel ball, m and the height of the drop, h were kept constant throughout the analysis in order to make it distinct and focus only on enhancing the generated output voltage from the piezoelectric.

A. Piezoelectric Characterization, Supporting Base and Rectification

Naturally, in the free-fall event that uses a spherical mass, it is most likely to see that the mass will keep bouncing until its momentum decays to zero across time. The same analogy is applicable in this experiment. The steel ball mass that has been impacted on the piezo generates the highest instantaneous output voltage for the first impact and the impact will instantly decrease until it stops bouncing. According to the $\frac{1}{2}mv^2$, the highest kinetic energy, K_E of the ball is when it impacts on the piezoelectric for the first time. However, this energy will slowly fade away after the initial impact as the potential energy, P_E of the mass is not the highest as before the falling. Figure 8 illustrates the whole process in a single waveform. As shown in Figure 8, the highest output voltage produced from the piezoelectric with a force of $490\mu J$ is $30.6V_{max}$, which is the output obtained from the very first impact. The rest of the results generated from the momentum of the ball were neglected since it is unpredictable and literally very small.

One of the ways to increase the resulted output voltage from the piezoelectric is by increasing the strain displacement of the transducer itself. Based on the configuration stated in the previous section, the piezoelectric was placed on two different setups; one was placed directly on the flat surface workspace, while another one was gummed on to the proposed supporting base. Figure 8 and 9 show the generated output voltage captured by the

oscilloscope when the piezo is placed without and with the supporting base respectively. In these figures, as can be seen under the Measurement section, the reading for the instantaneous output voltage, V_{max} and V_{min} have been highlighted in yellow and red box respectively. For instance, V_{max} is the positive cycle while V_{min} is the negative part of the sine wave. From these figures, the one with the supporting base, which is in Figure 9, is able to produce higher output voltage, $V_{max}= 35.0V$ compared to the one without the supporting base, $V_{max}= 30.6V$ with the potential difference of nearly 5V. In addition, the negative cycle from the first initial impact also becomes higher from $-4.4V_{min}$ (without the base) to $-10.1V_{min}$ (with the base). Therefore, this verifies that the generated output voltage from the piezoelectric for both cycles can be enhanced by increasing the displacement of the piezo. This is due to the characteristic of the piezoelectric based on the relationship between the electric displacement, D_3 resulted from the strain, S_3 based on the mathematical expression of $D_3 = d_{33}S_3$, where S_3 is the strain of the piezoelectric along the x-axis while d_{33} is the piezoelectric strain constants that exist from the vertical impact displacement. Based on the equation, when d_{33} is constant, the strain S_3 will affect the changes on the electrical displacement as D_{33} is directly proportional to the strain, S_3 . Therefore, for the rest of the experiments, the transducer was tested by using the supporting base to enhance the generated output voltage.

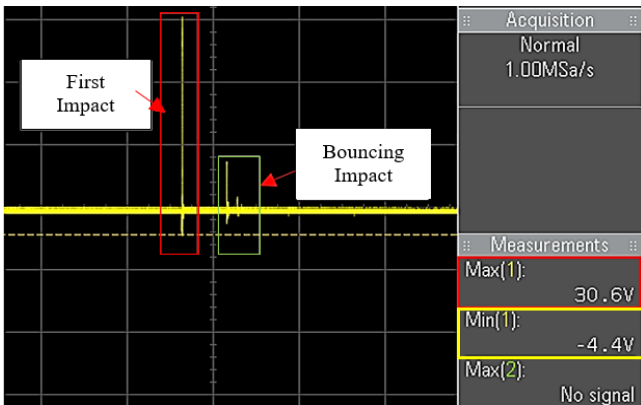


Figure 8: Generated AC output voltage of piezoelectric without the disk's setting base

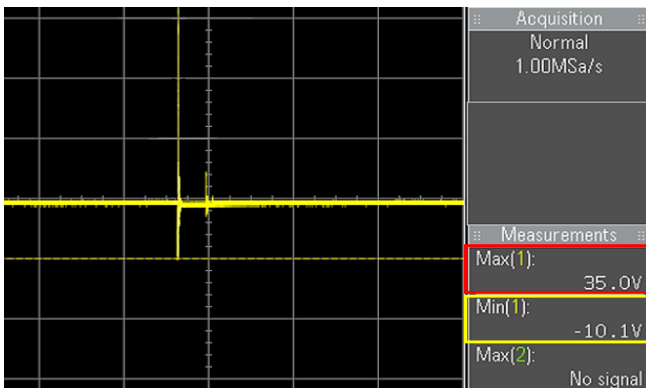


Figure 9: Generated AC output voltage of piezoelectric with the disk's supporting base.

In order to utilize this harvested output voltage, the AC signals from the piezo need to be rectified first into DC form. Figure 10 shows the rectified output waveform captured by the oscilloscope in open circuit connection without connecting it to any external load. The AC signals

from the piezoelectric were rectified using conventional full-wave bridge rectifier. From the figure, the negative part of from the AC signal has been inverted to the positive part of the waveform. Supposedly, an ideal DC voltage should be in the form of straight horizontal line. However, in this case, the input supplied to the rectifier from the harvester was only at an instance. Thus, the rectified output voltage captured by the oscilloscope also existed only during the free-falling event.

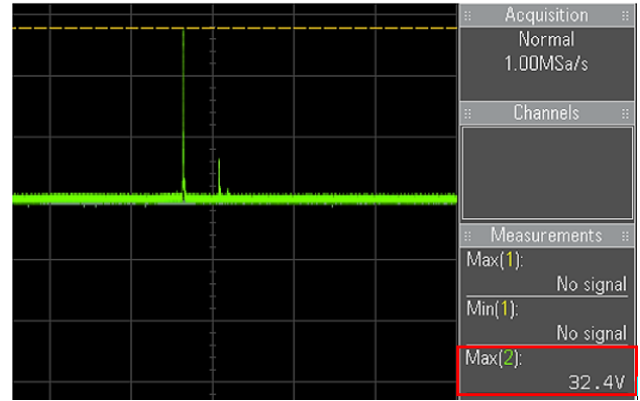


Figure 10: Generated rectified output voltage of the full-wave bridge rectifier.

B. Diode Classification Performance Analysis

As a starting point in looking for an area to reduce the power dissipation during the conversion process of the AC to DC, full-wave bridge rectifier was selected as it was able to utilize both negative and positive cycle of the signals. An analysis on the performances of full-wave bridged rectifier circuit using different types of diodes have been conducted. The rectifier was constructed using three different types of diodes with different internal characteristic to analyze the performance and its efficiency. The proposed diodes were Schottky (1N5819), Silicon (1N4007) and Zener (1N4728) and their specifications are presented in Table 2.

Table 2
Diode specifications

Parameter	Description		
Manufacturer	Vishay	Vishay	M.C.C
Product number	1N4007	1N5819	1N4728
Diode Type	Silicon	Schottky	Zener
Forward voltage $V_f(V)$	1.1	0.6	1.2
Forward current $I_f(A)$	1.0	1.0	0.2
Peak reverse voltage (V)	1000	40	75
Peak reverse current (mA)	0.000005	0.001	0.0001
Diameter (mm)	2.7	2.7	2.80
Length (mm)	5.2	5.2	4.5

The generated open circuit output voltage of the full-wave bridge rectifier shown in Figure 10 is equal to 32.4Vmax when the rectifier was constructed using 1N5819 Schottky diode. However, when the transducer was directly connected to the oscilloscope; excluded the rectifier circuit, the resulted output captured was 35.0Vmax. From here, it can be said that there was some voltage drop across the diode during the rectification process. Based on the loop equation of the voltage theorem, $V_o = V_s - V_D$, the output voltage, V_o is equal to the voltage difference of source voltage, V_s and the voltage drop across the diode, V_D . This explained why the generated output voltage was not the same as the supplied input voltage.

The efficiencies of the rectification system were analyzed in

term of power. In order to calculate the power, the circuits were connected to a decade resistance box with range of 0Ω to 10MΩ to vary the load to find the optimum resistive load for the harvester. Figure 11 shows the voltage curves of the proposed diodes performance in a single impact weight-drop analysis on the piezoelectric. From the graph, the full-wave rectifier constructed of Zener diodes has the lowest resulted output voltage of at least 19.09% compared to the resulted output voltage of rectifier constructed with Schottky and Silicon diode. For the other two diodes, the rectifier constructed with Schottky diode is slightly higher compared to the one constructed using Silicon with 0.42% difference, turns out that there is only a small potential difference between this two. From the same plotting curves, both of Silicon and Schottky rectifier begin to saturate at the magnitude of 31Vmax.

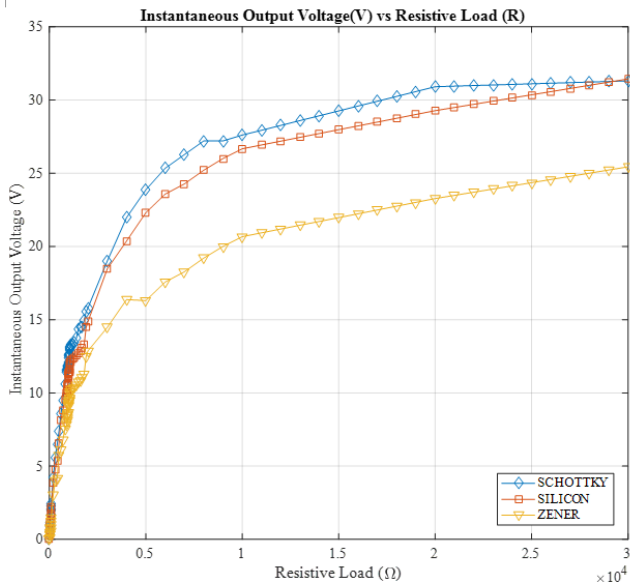


Figure 11: Instantaneous peak voltage (V) vs Resistive load (Ω) comparing diode characteristic

The circuit output power can be easily calculated based on the power equation law, $P_L = V_L \cdot I_L$, as the value of the rectified output voltage and the value of the load resistance can be measured, where V_L and I_L is the output voltage and current across the load respectively. Figure 12 shows the plotted output power of these rectifier circuit for each diode specification. Since the output load is a resistance, according to the Ohmic's Law, $V = IR$, the voltage of the load is directly proportional to the output current. We can simply get the value of current, I_L according to $I_L = \frac{V_L}{R_L}$. All of the circuits have the most optimum output power at 1.1kΩ resistive load, which can be seen from the peak of the curves. Similar to the previous voltage performance, Schottky diode still took the lead in term of power. It still generated the highest optimum output power of 160mW, leading the Silicon and Zener with 17.18% and 43.55% accordingly.

Then, the circuit was analyzed in term of efficiency, η . It can be calculated from the ratio of the output power, P_{DC} to the total input Ac power, $P_{AC} = P_L + P_D$, where P_D is the losses across the diode during rectification, which can be expressed by Equation (6) and (7). In this case, the efficiencies for the harvested power from the full-wave bridge rectifier for each diode were 67.2%, 58% and 34.86%

for Schottky, Silicon and Zener, respectively. It can be concluded that every each of the elements in the power conditioning circuit, in this case; forward voltage of a diode rectifiers, filter capacitance and resistive load, have their own parasitic consumption that will affect the efficiency of the circuit. Voltage supplies must be higher than the forward voltage V_f of a diode in order for the diode to be turned on. Otherwise, the current is unable to flow through the diodes in forward biased, resulting the circuits to be open circuit. Besides, the voltage that drops across the diodes also affects the power losses of the rectifier. Therefore, to enhance the extracted power, the V_f value should be as low as possible to reduce the power loss in the rectifying diodes. The outcome from this analysis has been tabulated in Table 3.

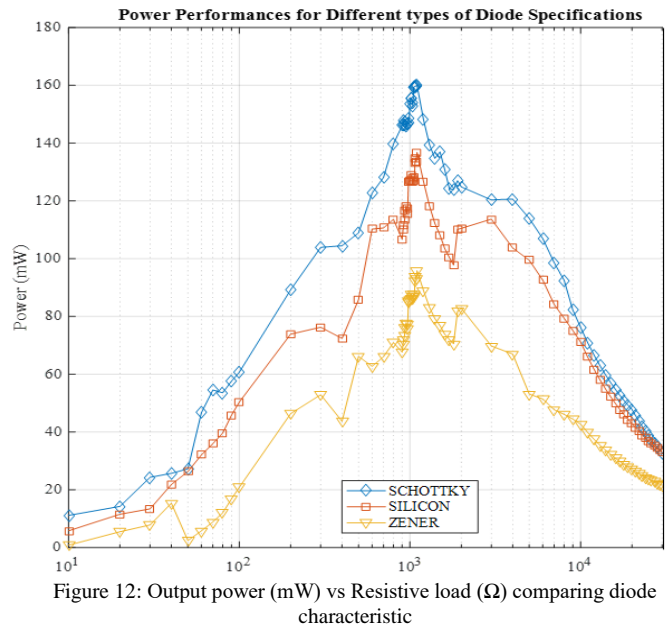


Figure 12: Output power (mW) vs Resistive load (Ω) comparing diode characteristic

$$\eta = \frac{P_{DC}}{P_L + P_D} \tag{6}$$

$$\eta = \frac{V_{DC} \cdot I_{DC}}{V_L \cdot I_L + R_D \cdot I_L^2} = \frac{V_{DC}^2}{V_L^2} \cdot \frac{1}{1 + \left(\frac{R_D}{R_L}\right)} \tag{7}$$

Table 3
Results of Full-Wave Rectifier Using Different Rectifier Types

Parameter	1N5819	1N4007	1N4728
Max. peak output voltage(V)	33.73	32.23	25.97
Opt. peak output voltage (V)	13.27	12.33	10.07
Optimum resistor load(kΩ)	1.1	1.1	1.1
Opt. output power (mW)	160	136.79	95.82

C. Rectifier Comparison

Next, the experimental analysis was followed by constructing the proposed rectifier circuits; half-wave, full-wave bridge, half-wave and full-wave voltage doubler using Schottky diodes in order to enhance their efficiencies. The configurations parameters still remain constant as in the previous test. All of the proposed circuits are consisted of 1N5819 Schottky diodes, an external wide range resistive decade box and an electrolytic capacitor filter, C_f that are used to filter the ripple signal. For specialized rectifier; half-wave and full-wave voltage doubler, they have an extra

electrolytic capacitor to store the voltage at each half cycle. These filter capacitor, C_f is one of the factors that affect the performances of regulating the output voltage by removing the ripples signal from the rectified output voltage.

Previously, there were four rectifier topologies to be analyzed in these experiments. Later, it was found that half-wave voltage doubler circuit configurations were not suitable to be interfaced with only one impact input signal application. This is due to the working principles of the circuit itself. It should be pointed out that the circuit has been tested working by directly connected it with an AC power sources from a step-down transformer with and output voltage of $7.7V_{AC}$. Both of the supplied voltage, V_S and the regulated output voltage, V_{OUT} were captured in channel 1 and channel 2 of oscilloscope respectively as shown in Figure 13. The yellow AC waveform is the supplied voltage with the operating frequency of 50Hz from the transformer with 5.00V/division. This half-wave voltage doubler was able to boost up the output voltage up to 15.3V as shown by the straight green DC line with 10.0V/division. The waveform was captured in 50ms time scales.

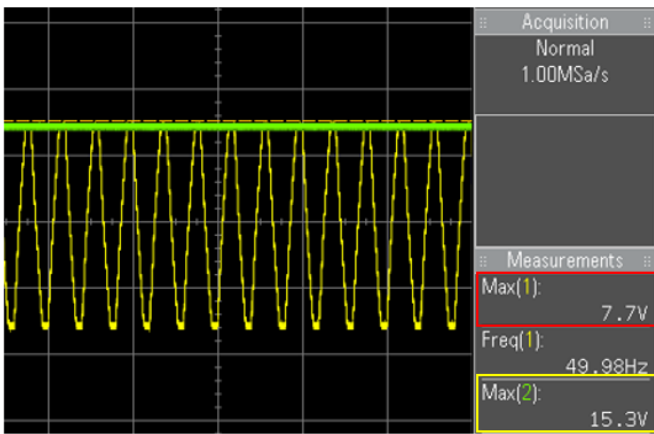


Figure 13: The input and output signals for half-wave voltage doubler

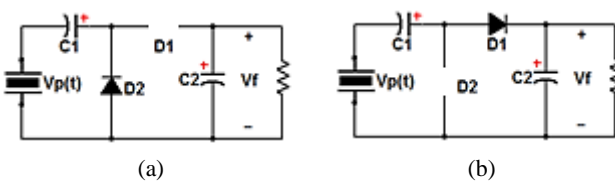


Figure 14: Working operation of Greinacher circuit

These circuit has been analyzed and studied on how it works. From the observations, the reason was discussed by comparing their performance on the continuous and single pulse input source. It was found that the main factor that causes this to happen was due to the arrangement of the storage capacitor C_1 and C_2 of this circuit. In each half cycle of the input signal, Diodes D_1 and D_2 were conducted simultaneously and they were never conducted at the same time. When this rectifier circuit was connected directly to the continuous AC sources, the diodes had the conducting period to store the energy into C_1 and C_2 . Besides, the magnitude of the continuous AC signal for the negative and positive part were the same compared with the one generated from the piezoelectric. Therefore, when capacitor C_1 released the stored voltage obtained from the first half cycle at the second half, the released stored voltage added up together with the negative half cycle, producing twice the amount of the supplied voltage. However, different

situations occurred when the input source was from one single impact piezoelectric transducer. For the first half cycle, when the piezo was impacted by the steel ball, diode D_2 was forward biased, while D_1 was reverse biased (open circuit) and vice versa for the next half cycle as shown in Figure 14. The cumulative voltage combined from the negative and positive cycle will never be able to produce twice the amount of the positive magnitude since the negative part of the transducer is literally smaller than the positive part. Therefore, the results from this test were not included during the comparison of the performances of the rectifier topologies. As can be seen from Figure 15 and 16, the legends consist of the results from half-wave, full-wave bridge and full-wave voltage doubler only.

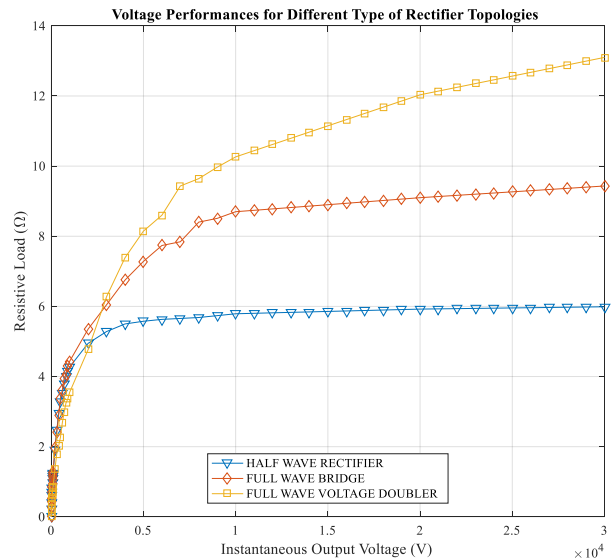


Figure 15: Instantaneous peak voltage (V) vs Resistive load (Ω) comparing rectifier configuration

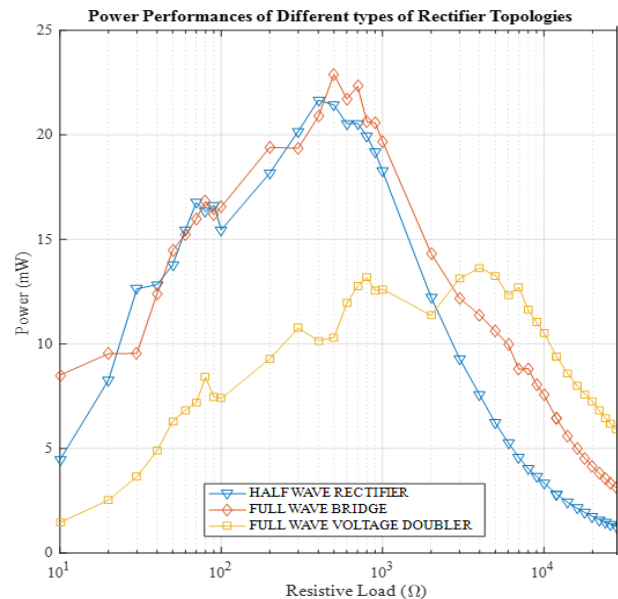


Figure 16: Output power (mW) vs Resistive load (Ω) comparing rectifier configuration

Figure 15 shows the results of the rectified output voltage of the proposed rectifiers. It was observed that the generated output voltage of the rectifier increased linearly and began to saturate when the resistance is higher than $10k\Omega$. This is due to the output voltage, $V = IR$, where voltage V is directly proportional to the resistive load R . Therefore, as

the resistivity gets higher, the generated output voltage increases also. By comparing the resulted output voltage for each rectifier topologies in Figure 15, it can be seen that at least there were 4V potential difference between each of them. However, an ideal voltage doubler is supposed to produce twice the magnitude of a conventional full-wave bridge rectifier. Again, this is due to the working principle of this rectifier and the generated voltage from the harvester itself. The negative half cycle generated from the harvester was too small to be able to produce output voltage two times higher than the positive cycle magnitude. Nevertheless, in this application, full-wave voltage doubler was still able to produce higher output voltage compared with the rest. The generated output voltage from half-wave rectifier was the lowest because of the diode clipped the negative part of the signal.

Figure 16 presents the performances of the proposed rectifiers in term of power against the resistive impedances to find the optimum resistive load for these circuits. Before this, the difference diodes specs with same rectifier configurations; full-wave bridge, had the same optimum resistive load at 1.1k Ω . However, this time, the optimum resistive load for each rectifier was different from each other. For half-wave and full-wave bridge rectifiers, their optimum resistive load was at around 500 Ω . Whereas, for full-wave bridge rectifier, it looks like there were two peaks when it was at the optimum level. The highest peak was still at 1.1k Ω . As illustrated by this graph, the generated output power for full-wave voltage doubler, 13.335mW was the lowest although it was the highest when comparing the rectifiers in term of output voltage. This is because of the power equation relationship, $P = IV$, where power P is directly proportional to the current, I . Ideally, in the same system, the total power in, P_{IN} is the same as the total output power P_{OUT} . In addition, based on the Ohmic's Law, voltage is directly proportional to the load and the current. Hence, when the rectifiers doubling up the output voltage twice the amount of the voltage supplied, actually, the current was being cutting down at least the same amount in order to maintain the law of the power equation. Although, the generated output voltage was twice the amount of the input signal, the output power still remained the same as the input power, $P_{IN} = P_{OUT}$. This is the reason why the resulted output power of voltage doubler was the lowest at this point. Therefore, in term of performances, the voltage doubler has the least efficiency compared to the other topologies. Table 4 summarizes the results of these experiments.

Table 4
Results of full-wave rectifier circuit configuration of traditional rectifier and voltage doubler.

Parameter	Full Wave Bridge	Delon Circuit
Max. peak output voltage(V)	9.1	13.10
Opt. peak output voltage (V)	3.38	4.52
Optimum resistor load(k Ω)	0.5	1.1
Total energy in capacitor (nJ)	571.22	733.5
Opt. output power (mW)	23	13.335

VI. CONCLUSION

Series of experimental evaluation with respect to the efficiency of rectifying circuit on impact-based piezoelectric energy harvester system had been conducted and discussed in this paper. The aim of these studies is to enhance the

optimum output power of the system. A piezoelectric transducer that has been impacted vertically with a velocity of 3.13156m/s has been able to generate an instantaneous peak voltage of 35V from 50mm high in open circuit configuration. In order to make the generated energy usable to power up the dc regulated electronic device, some rectifier topologies have been tested. From a branch of AC-DC converter available, half-wave, full-wave bridge, half-wave voltage doubler and full-wave voltage doubler rectifier have been selected in this test. Firstly, as the rectifier is mainly the composition of number of diodes, the voltage rectifier circuit were optimized by varying the values of the forward voltage of the diodes. Three different diodes have been selected, and it was found that Schottky diode has the highest performance compared to Silicon, and Zener. Secondly, a test on the comparison of the efficiency and generated output voltage and power of the selected rectifiers have been done. Both the half-wave rectifier and the Greinacher voltage doubler are not suitable to be used for impact-based excitation technique due to their working operations. In particular, the full-wave bridge rectifier circuit shows the highest power efficiency of 23mW compared to full-wave voltage doubler circuit with 13.335mW; although it is able to generate twice the voltage of full-wave bridge rectifier.

ACKNOWLEDGMENT

The corresponding author appreciates the Universiti Teknikal Malaysia Melaka (UTeM) sponsored by "UTeM Zamalah Scheme" for the financial support during her Master Degree study at the Universiti Teknikal Malaysia Melaka.

REFERENCES

- [1] H. Yu, Q. Yue, and H. Wu, "Power management and energy harvesting for indoor photovoltaic cells system," in *2011 Second International Conference on Mechanic Automation and Control Engineering*, 2011, pp. 521–524.
- [2] K. Khan, M. Ahmed, M. S. Parvez, and M. M. Hossain, "Scope of geothermal potential of Bangladesh: A review," in *2015 3rd International Conference on Green Energy and Technology (ICGET)*, 2015, pp. 1–4.
- [3] A. Zahedi, "A comprehensive review of operational analysis of wind turbines," in *2015 Australasian Universities Power Engineering Conference (AUPEC)*, 2015, pp. 1–5.
- [4] P. Oliveira, F. Taveira-Pinto, T. Morais, and P. Rosa-Santos, "Experimental evaluation of the effect of wave focusing walls on the performance of the Sea-wave Slot-cone Generator," *Energy Convers. Manag.*, vol. 110, no. Supplement C, pp. 165–175, 2016.
- [5] S. Roundy, P. K. Wright, and J. Rabaey, "A study of low level vibrations as a power source for wireless sensor nodes," *Comput. Commun.*, vol. 26, no. 11, pp. 1131–1144, 2003.
- [6] L. Atzori, A. Iera, and G. Morabito, "The Internet of Things: A survey," *Comput. Networks*, vol. 54, no. 15, pp. 2787–2805, 2010.
- [7] N. Khalil, M. R. Abid, D. Benhaddou, and M. Gerndt, "Wireless sensors networks for Internet of Things," in *2014 IEEE Ninth International Conference on Intelligent Sensors, Sensor Networks and Information Processing (ISSNIP)*, 2014, pp. 1–6.
- [8] M. Han, Y. C. Chan, W. Liu, S. Zhang, and H. Zhang, "Low frequency PVDF piezoelectric energy harvester with combined d31 and d33 operating modes," in *The 8th Annual IEEE International Conference on Nano/Micro Engineered and Molecular Systems*, 2013, pp. 440–443.
- [9] E. Arroyo, A. Badel, F. Formosa, Y. Wu, and J. Qiu, "Comparison of electromagnetic and piezoelectric vibration energy harvesters: Model and experiments," *Sensors Actuators A Phys.*, vol. 183, 2012.
- [10] A. D. T. Elliott, L. M. Miller, E. Halvorsen, P. K. Wright, and P. D. Mitcheson, "Which is better, electrostatic or piezoelectric energy harvesting systems?," *J. Phys. Conf. Ser.*, vol. 660, no. 1, p. 12128,

- 2015.
- [11] N. A. A. Nawir, A. A. Basari, M. S. M. Saat, N. X. Yan, and S. Hashimoto, "A Review on Piezoelectric Energy Harvester and Its Power Conditioning Circuit," *ARPN Journals*, 2018.
- [12] J. Y. (auth.), *An Introduction to the Theory of Piezoelectricity*, 1st ed. Springer US, 2005.
- [13] X. Xu, D. Cao, H. Yang, and M. He, "Application of piezoelectric transducer in energy harvesting in pavement," *Int. J. Pavement Res. Technol.*, 2017.
- [14] A. C. LINKS, "Wireless Sensor Networks: Maintenance-Free or Battery-Free?" Jan-2009.
- [15] P. Sarkar and S. Chakrabarty, "A compressive piezoelectric front-end circuit for self-powered mechanical impact detectors," in *2013 IEEE International Symposium on Circuits and Systems (ISCAS2013)*, 2013, pp. 2207–2210.
- [16] A. Tabesh and L. G. Fréchet, "An improved small-deflection electromechanical model for piezoelectric bending beam actuators and energy harvesters," *J. Micromechanics Microengineering*, vol. 18, no. 10, p. 104009, 2008.
- [17] M. Massarotto, A. Carlosena, S. Garriz, and J. M. Pintor, "An Impact Technique for Wide Band Characterization of Piezoelectric Accelerometers," in *2007 IEEE Instrumentation Measurement Technology Conference IMTC 2007*, 2007, pp. 1–6.
- [18] M.-C. Chure, L. Wu, K.-K. Wu, C.-C. Tung, J.-S. Lin, and W.-C. Ma, "Power generation characteristics of PZT piezoelectric ceramics using drop weight impact techniques: Effect of dimensional size," *Ceram. Int.*, vol. 40, no. 1, Part A, pp. 341–345, 2014.
- [19] G. Martínez-Ayuso, M. I. Friswell, S. Adhikari, H. H. Khodaparast, and C. A. Featherston, "Energy harvesting using porous piezoelectric beam with impacts," *Procedia Eng.*, vol. 199, no. Supplement C, pp. 3468–3473, 2017.
- [20] A. A. Basari *et al.*, "Study of the effect of mechanical impact parameters on an impact-mode piezoelectric ceramic power generator," *Ceram. Int.*, vol. 41, no. 9, Part B, pp. 12038–12044, 2015.
- [21] M. F. V. F. D. Alghisi S. Dalola, "Triaxial ball-impact piezoelectric converter for autonomous sensors exploiting energy harvesting from vibrations and human motion," *Sensors Actuators A Phys.*, vol. 233, no. Supplement C, pp. 569–581, 2015.
- [22] T. Apostolopoulos and A. Vlachos, "Application of the Firefly Algorithm for Solving the Economic Emissions Load Dispatch Problem," *Int. J. Comb.*, vol. 2011, pp. 1–23, 2011.
- [23] S. N. H. K. Eric Simon Yuichiro Hamate, "3D Vibration Harvesting Using Free Moving Ball in PZT Microbox," *Power MEMS*, pp. 3–6, 2010.
- [24] A. M. Abdal-Kadhim, K. S. Leong, and L. K. Tee, "Impact based piezoelectric energy harvesting: effect of single step's force and velocity," *J. Telecommun. Electron. Comput. Eng.*, vol. 8, no. 5, pp. 125–129, 2016.
- [25] A. A. Mustapha, K. Leong, and N. M. Ali, "Piezoelectric energy harvesting rectifying circuits comparison," *ARPN J. Eng. Appl. Sci.*, vol. 11, no. 10, pp. 6361–6365, 2016.
- [26] D. Motter, J. V. Lavarda, F. A. Dias, and S. da Silva, "Vibration energy harvesting using piezoelectric transducer and non-controlled rectifiers circuits," *J. Brazilian Soc. Mech. Sci. Eng.*, vol. 34, no. SPE, pp. 378–385, 2012.
- [27] A. A. Basari *et al.*, "Evaluation on mechanical impact parameters in piezoelectric power generation," in *2015 10th Asian Control Conference (ASCC)*, 2015, pp. 1–6.
- [28] A. Tabesh and L. G. Frechette, "A Low-Power Stand-Alone Adaptive Circuit for Harvesting Energy From a Piezoelectric Micropower Generator," *IEEE Trans. Ind. Electron.*, vol. 57, no. 3, pp. 840–849, Mar. 2010.
- [29] Y. K. Ramadass and A. P. Chandrakasan, "An Efficient Piezoelectric Energy Harvesting Interface Circuit Using a Bias-Flip Rectifier and Shared Inductor," *IEEE J. Solid-State Circuits*, vol. 45, no. 1, pp. 189–204, Jan. 2010.